

## 4D gravity changes associated with the 2005 eruption of Sierra Negra volcano, Galápagos

Nathalie Vigouroux<sup>1</sup>, Glyn Williams-Jones<sup>1</sup>, William Chadwick<sup>2</sup>, Dennis Geist<sup>3</sup>,  
Andres Ruiz<sup>3</sup>, and Dan Johnson<sup>4</sup>

### ABSTRACT

Sierra Negra volcano, the most voluminous shield volcano in the Galápagos archipelago and one of the largest basaltic calderas in the world, erupted on October 22, 2005 after more than 25 years of quiescence. GPS and satellite radar interferometry (InSAR) monitoring of the deformation of the caldera floor in the months prior to the eruption documented extraordinary inflation rates (1 cm/day). The total amount of uplift recorded since monitoring began in 1992 approached 5 m at the center of the caldera over the eight days of the eruption the caldera floor deflated a maximum of 5 m and subsequently renewed its inflation, but at a decelerating rate. To gain insight into the nature of the subsurface mass/density changes associated with the deformation, gravity measurements performed in 2005, 2006, and 2007 are compared to previous measurements from 2001–2002 when the volcano underwent a period of minor deflation and magma withdrawal.

The residual gravity decrease between 2001–2002 and 2005 is among the largest ever recorded at an active volcano ( $-950 \mu\text{Gal}$ ) and suggests that inflation was accompanied by a relative density decrease in the magmatic system. Forward modeling of the residual gravity data in 4D (from 2002 to 2005) gives an estimate of the amount of vesiculation in the shallow sill required to explain the observed gravity variations. Geochemical constraints from melt inclusion and satellite remote-sensing data allow us to estimate the pre-eruptive gas content of the magma and place constraints on the thickness of the gas-rich sill necessary to produce the gravity anomalies observed. Results suggest that reasonable sill thicknesses (700–800 m) and bubble contents (10–50 volume %) can explain the large decrease in residual gravity prior to eruption. Following the eruption (2006 and 2007), the deformation and gravity patterns suggest re-equilibration of the pressure regime in the shallow magma system via a renewed influx of relatively gas-poor magma into the shallow parts of the system.

### INTRODUCTION

Information on mass changes in the subsurface over time can be obtained from microgravity surveys. In volcanic systems, changes in magma supply rate (influx or withdrawal), changes in the vesicularity of magma, and changes in the size or depth of a hydrothermal system can affect the gravity field measured at the surface (e.g., Tiede; [Gottsmann et al., 2006](#)). Typically, gravity variations on the order of hundreds of  $\mu\text{Gals}$  are recorded over years to decades and are associated with vertical deformation on the order of a few centimeters to a few meters (e.g., [Rymer, 1996](#); [Battaglia et al., 1999](#)). When combined with simultaneous data on elevation change (using

GPS or InSAR), microgravity surveys allow us to investigate the causes of ground deformation in active volcanic areas and evaluate the likelihood of an impending eruption (e.g., [Yokoyama and Tajima, 1957](#)) at a variety of volcanoes, from large silicic calderas (e.g., Campi Flegrei; [Berrino et al., 1984](#)) to composite stratovolcanoes (e.g., Merapi; [Jousset et al., 2000](#)) and basaltic calderas (e.g., Kilauea; [Johnson, 1992](#)). Logistical constraints usually limit the spatial and temporal coverage of the gravity network in remote volcanic area. However, combined with high-precision, continuously recorded ground deformation data, even sparse microgravity data can provide important information on the source of physical unrest at a volcano (e.g., [Kauahikaua and Miklius, 2003](#)).

Manuscript received by the Editor 28 February 2008; revised manuscript received 26 May 2008; published online 20 November 2008.

<sup>1</sup>Simon Fraser University, Department of Earth Science, Burnaby, British Columbia, Canada. E-mail: nvigouro@sfu.ca; glynwj@sfu.ca.

<sup>2</sup>Oregon State University-NOAA, Newport, Oregon, U.S.A. E-mail: william.w.chadwick@noaa.gov.

<sup>3</sup>University of Idaho, Department of Geological Sciences, Moscow, Idaho, U.S.A. E-mail: dgeist@uidaho.edu; gorkiruiz@hotmail.com.

<sup>4</sup>Deceased.

© 2008 Society of Exploration Geophysicists. All rights reserved.

Sierra Negra is an active basaltic shield volcano located in the Galápagos archipelago, a volcanic hotspot in the eastern Pacific Ocean (Figure 1). It is one of the most active volcanoes in the Galápagos and is by far the most voluminous. Sierra Negra has one of the largest calderas of any basaltic volcano on the planet ( $10 \times 9$  km; Wood, 1984). The caldera floor has been uplifted by up to 100 m in the southwest corner as a result of repeated slip along a sinuous fault system (Figure 2; Reynolds et al., 1995; Chadwick et al., 2006). The northeast side of the fault block forms a dip slope, resulting in a trapdoor/asymmetric geometry (Lipman, 1997).

On October 22, 2005, Sierra Negra erupted more than  $150 \times 10^6$  m<sup>3</sup> of aphyric (crystal-free) basaltic lava (Geist et al., 2008). Uplift of more than 2 m in the center of the caldera was recorded by continuous GPS over the three years preceding the October 2005 eruption (Chadwick et al., 2006). The total inflation (estimated to be 5 m since 1992) prior to eruption is the largest ever recorded at a basaltic caldera (Chadwick et al., 2006). Monitoring of the deformation provides information about the rate of volume increase in a subsurface magma chamber and places constraints on the geometry and depth of this reservoir but alone cannot determine the exact processes causing inflation.

In this contribution, we present gravity data collected prior to and following the October 2005 eruption. In combination with previously published microgravity data on Sierra Negra (Geist et al., 2006), a time-series analysis of both microgravity and continuous deformation data offers insight into the subsurface processes associated with the 2005 eruption. We use previously published models of the magma reservoir geometry obtained from the inversion of deformation data (Amelung et al., 2000; Chadwick et al., 2006; Geist et al., 2006; Yun et al., 2006) to model the gravity changes.

## METHODS

The theory and field practice for microgravity monitoring in volcanic areas has been well described in the literature (e.g., Rymer and Brown, 1989; Rymer, 1996) and therefore will be only summarized briefly here. The gravity network at Sierra Negra is sparse because of the extremely difficult access to the caldera and rough terrain (at least ten hours of hiking is required to visit three gravity stations in

the center of the caldera). Our efforts were thus focused on measurements at the center of deformation in the middle of the caldera (Figure 2). Stations were visited in June 2005, four months prior to the eruption, and in June 2006 and 2007. These data are used in conjunction with earlier gravity surveys in 2001 and 2002 (Geist et al., 2006). All surveys were conducted during the dry season in June. This strategy is designed to limit the effect of water-table fluctuations on the gravity measurements. Although precise water-table effects were not quantified, given the large gravity variations observed, any water-related effects on the same order as those observed at other calderas (e.g., up to 60  $\mu$ Gal at Yellowstone; Battaglia et al., 2003) would fall within the error of our measurements.

Two LaCoste and Romberg model G gravity meters (instruments G-127 and G-209) were used over the course of the surveys at Sierra Negra. The G-209 meter was used for the 2001–2002 (Geist et al., 2006) and June 2005 surveys, whereas the G-127 meter was used during the more recent surveys in 2006 and 2007. The G-209 meter is equipped with a galvanometer and thus the reported microgravity measurements for a given station are taken from at least two individual readings. In contrast, the G-127 meter is equipped with an Aliod electrostatic feedback nulling system allowing for repeated in situ measurements (at 2 Hz) without the need for user input. Both instruments were calibrated on a Palm Desert (California) gravity line and the data presented here are corrected to the G-127 meter.

When time permitted, each station was visited twice during a survey loop and some stations were measured on two days of the campaign. Our raw gravity measurements are corrected for earth tide, ocean loading, and elevation effects (Table 1). The Bouguer corrected free air gradient (BCFAG) = a free air gradient (FAG) of  $-308.6 \mu$ Gal/m plus an infinite-slab Bouguer correction of  $117.3 \mu$ Gal/m, assuming a surrounding rock density of  $2.8 \text{ g/cm}^3$ , as used for the correction. The resulting corrected gravity measurement is referred to as the residual gravity. Instrumental drift was negligible over the survey periods. Error in the residual gravity measurements is as follows; the standard deviation ( $1\sigma$ ) in the residual gravity averaged over 1 minute and measured over 6–10 minutes at a given station is less than  $5 \mu$ Gal for the G-127 meter. The standard deviation at a given station over the course of one campaign is on the order of  $100 \mu$ Gal because of the difficult conditions experienced by the instruments during transport over rugged terrain. The closure error (difference in the residual gravity measurements made at the base

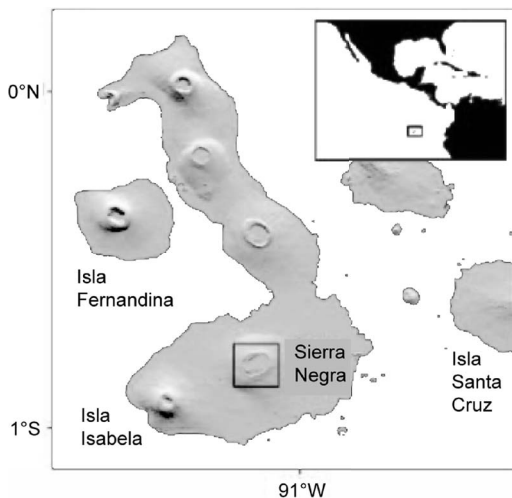


Figure 1. Digital elevation map of the Galápagos archipelago showing the locations of the Sierra Negra and Fernandina calderas (modified after Yun et al., 2006).

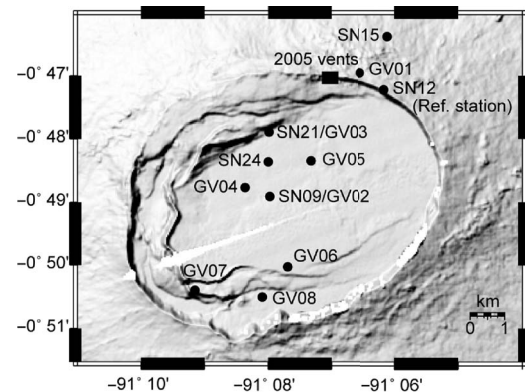


Figure 2. Digital elevation map of the summit area of Sierra Negra showing the location of the gravity (SN) and continuous GPS (GV) stations referred to in this study. The eruptive vents from 2005 also are shown.

station, SN12, in one day) was also taken into account. Sources of error that factor into the residual gravity measurements include uncertainty in the vertical component of deformation as measured by continuous GPS at most of the gravity benchmarks and uncertainty in the extrapolation of deformation rates to benchmarks at which no GPS data are available. We also take into account possible variation in the FAG gradient of up to  $\pm 10\%$  (Tsuboi, 1983).

### Gravity and deformation results

Deformation data for Sierra Negra extend back to 1992 with satellite radar interferometry (InSAR) studies indicating inflation of 2.5 m from 1992 to 1999, with maximum uplift rates of 60 cm/yr (Amelung et al., 2000). The InSAR data were inverted to model the magma body and indicated a 2.1–2.3-km-deep sill located beneath the center of the caldera (Amelung et al., 2000).

In June 2001 and June 2002, GPS campaigns covered a network of 14 to 26 stations at Sierra Negra (Geist et al., 2006). They reported a greatly decreased rate of inflation during the first year, with a maximum uplift rate of 7 cm/yr, followed by 9 cm of deflation over the next 1.5 years. This period of deflation was accompanied by a 50  $\mu\text{Gal}$  decrease in the residual gravity observed in the northern part of the caldera (station SN21, relative to SN12 on the caldera rim; Figure 2). Geist et al. (2006) suggest the combined deflation and decrease in gravity was linked to an episode of magma withdrawal from the shallow magma reservoir, probably into the deeper parts of the plumbing system. From the GPS data, the best-fit geometry for the deflating magma body was found to be a sill with horizontal dimensions of  $5.3 \times 3.0$  km and a depth comparable to that modeled by the InSAR data (2.1–2.3 km). Based on this geometry, the magma body would have contracted in volume by  $4.1 \times 10^6$  m<sup>3</sup> (Geist et al., 2006).

In June 2002, a network of continuous GPS stations was installed on the caldera floor of Sierra Negra, with one station located on its northeast rim (Figure 2). The GPS network continued to record the deflation, which began in 2000–2001 at a rate of  $-9.1$  cm/yr, and then in April 2003 the system switched back to inflation (Chadwick et al., 2006). Between April 2003 and the October 2005 eruption, station GV02, located near the center of the caldera, recorded 2.2 m of uplift. Horizontal north-south extension (GV03–GV06) amounted to 1.4 m over the same time period. An  $m_b$  4.6 earthquake occurred on April 16, 2005 along with 84 cm of vertical slip on the south end of the intracaldera fault system but this event did not interrupt the pattern of inflation (Chadwick et al., 2006). This suggests that despite faulting in the roof of the magma reservoir, the internal pressure in the subsurface reservoir was apparently unaffected. Unfortunately, no gravity data were collected between June 2002 and June 2005 but such high inflation rates prior to an eruption are generally associated with continuous magma influx into the shallow reservoir (Johnson, 1992).

Gravity measurements made four months prior to the October 2005 eruption at the center of the caldera (SN09) show a decrease in residual gravity (relative to the reference station SN12) of up to 950  $\mu\text{Gal}$  compared to measurements from 2001 and 2002 (Figure 3). The residual gravity decrease becomes less pronounced toward

the caldera rim, with station SN21 recording a 450  $\mu\text{Gal}$  decrease relative to 2001–2002. The change in residual gravity on the flank of the caldera (station SN15) is negligible between 2001–2002 and 2005 (Figure 3). This suggests that the residual gravity anomaly and, hence, the area of mass change/density decrease prior to the eruption, was restricted to the interior of the caldera.

Gravity measurements made eight and twenty months after the 2005 eruption reveal an increase in residual gravity relative to June 2005 of up to 1000  $\mu\text{Gal}$ , again centered on SN09 (Figure 3). For SN09, this represents a slightly higher residual gravity value than those recorded in 2001–2002. For all other stations, the residual gravity measured in June 2007 is lower than the 2001–2002 levels by up to 350  $\mu\text{Gal}$  (SN15). Given the error in the measurements, stations SN24 and SN21 show no definite pattern of residual gravity change from immediately preceding, to after the eruption (June 2005–June 2007). Station SN15, however, shows a clear residual gravity decrease following the 2005 eruption. The change in the relative difference in residual gravity among stations (e.g., SN09–SN24) prior to and following the eruption suggests a shift in the mass distribution at depth as a result of the eruption. Finally, the relative changes in residual gravity measured at SN21 (north edge of the caldera floor) over the entire period, are greater (although within error) than the changes measured at SN24 (the station located between SN09 and SN21) indicating that the residual gravity change was radially asymmetric.

Table 1 Summary of gravity and deformation data at Sierra Negra

Year	2001*		2002*		2005		2006		2007	
Instrument used	G-209		G-209		G-209		G-127		G-127	
Station	Raw gravity (mGal)		Error		Error		Error		Error	
SN09	32.89	0.01	32.91	0.01	31.62	0.11	32.90	0.05	32.84	0.06
SN21	34.36	0.01	34.35	0.01	33.78	0.13	33.99	0.05	34.01	0.06
SN24	34.91	0.01	34.90	0.01	34.35	0.11	34.79	0.05	34.74	0.04
SN15	34.03	0.01	33.98	0.01	33.96	0.04	-	-	33.56	0.06
	Elevation (m)		Error		Error		Error		Error	
SN09	952.395	0.013	952.262	0.009	953.407	0.064	952.163	0.016	952.756	0.010
SN21	927.914	0.018	927.860	0.007	928.309	0.039	927.501	0.012	927.808	0.007
SN24	938.492	0.016	938.404	0.009	939.201	0.053	937.675	0.020	938.147	0.010
SN15	797.155	0.013	797.051	0.008	797.075	0.025	797.241	0.017	797.259	0.020
Time period	$\Delta g_{\text{max}}$ **	Error	$\Delta h_{\text{max}}$	Error	$(\Delta g/\Delta h)_{\text{max}}$					
2002–2005 (SN09)	-1067	113	1.15	0.06	-931					
2006–2007 (SN09)	71	79	0.59	0.02	119					

Raw gravity values are referenced to the base station SN12. Instruments have been cross-calibrated (referenced to G-127).

\* Data from Geist et al. (2006).

\*\* Corrected for elevation effects (BCFAG=  $-191.3$   $\mu\text{Gal/m}$ )

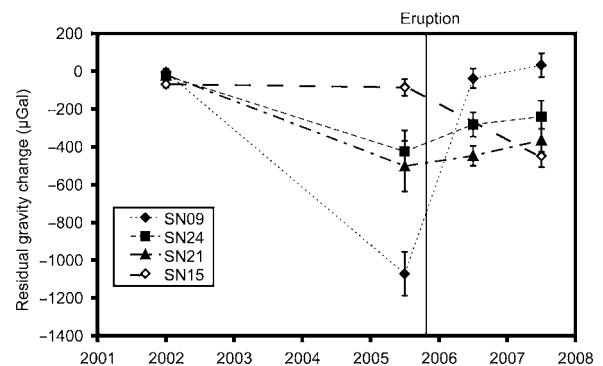


Figure 3. Residual gravity change (BCFAG corrected) recorded at all stations and referenced to June 2001. The October 2005 eruption is indicated. Error bars represent compounded errors from the sources discussed in the text.

DISCUSSION

The large decrease in residual gravity observed at SN09 and to a lesser extent at SN21 and SN24 preceding the 2005 eruption can be best explained in terms of either a mass or density decrease in the subsurface. At the time of the June 2005 gravity survey, the caldera floor was in a period of accelerating inflation (Chadwick et al., 2006). This rapid increase in elevation of the caldera floor has been interpreted as being caused by an increase in the volume of the subsurface magma chamber (Chadwick et al., 2006), which, given the subsequent eruption, could be due either to influx of magma into a shallow magma chamber or vesiculation of the residing magma or a combination of the two processes. To distinguish between these processes, we plot the residual gravity data on a  $\Delta g/\Delta h$  diagram (Rymer and Williams-Jones, 2000), which allows for better visualization of the processes responsible for the residual gravity changes (Figure 4). The maximum  $\Delta g/\Delta h$  gradient for the time periods of 2002–2005 and 2006–2007 (at station SN09) are plotted along with the theoretical FAG and the calculated BCFAG. The maximum gradient prior to the eruption (2002–2005) plots below both the FAG and BCFAG gradients indicating a decrease in mass and/or a decrease in density. The maximum gradient following the eruption (2006–2007) plots above both the FAG and the BCFAG indicating a mass increase and/or density increase. It is unlikely that magma withdrawal (mass decrease) was the dominant process during the time period of 2002–2005 because of the observed inflation leading up to the eruption. Therefore, the  $\Delta g/\Delta h$  gradient observed from 2002 to 2005 is best explained by magma vesiculation (density decrease).

To investigate the role of magma vesiculation in generating the large residual gravity decrease prior to the eruption, we model the shallow magma body using the program GRAV3D (GRAV3D, 2007) and solve for the density and thickness of the magma body needed to generate the maximum residual gravity change recorded

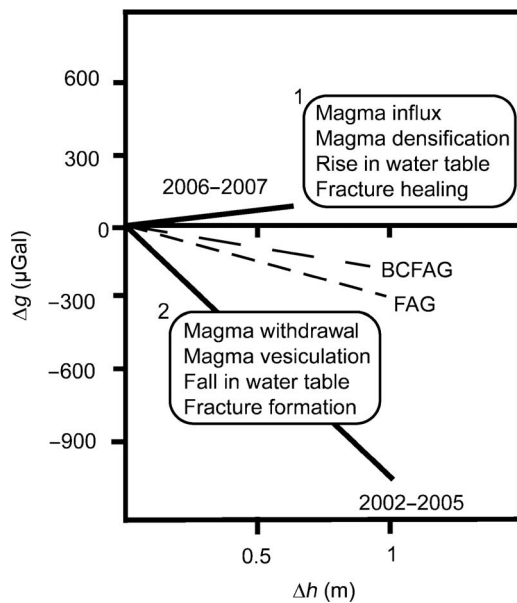


Figure 4. Maximum  $\Delta g/\Delta h$  gradient for the time period 2002–2005 and 2006–2007 (station SN09) and theoretical FAG ( $-308.6 \mu\text{Gal}/\text{m}$ ) and calculated BCFAG ( $-191.3 \mu\text{Gal}/\text{m}$ ). Scenario boxes 1 and 2 are for gradients that plot above the BCFAG and below the FAG lines, respectively.

from 2002 to 2005 at SN09. Inverse modeling of the gravity data to solve for the exact density of the causative body was not performed because of the limited spatial coverage of the gravity network. Forward modeling is appropriate because of the good control we have on the geometry of the chamber and its location.

Inverse modeling of the deformation data collected at Sierra Negra by both InSAR and GPS since 1992 suggests the deformation is controlled mainly by inflation and deflation of a shallow, sill-like magma body located at 2.1–2.3 km depth (top of the chamber) and having horizontal dimensions of  $5.3 \times 3.0 \text{ km}$  (Figure 5; Amelung et al., 2000; Chadwick et al., 2006; Geist et al., 2006). However, there is no constraint on the thickness of the body, which could range from hundreds of meters to  $>1 \text{ km}$  (Yun et al., 2006). The chamber geometry is assumed to remain constant between 2002 and 2005. The change in the volume of the chamber of  $3.6 \times 10^7 \text{ m}^3$  between June 2002 and 2005 (Chadwick et al., 2006) will have an effect on the gravity field but because this volume increase represents  $\ll 1\%$  of the total volume of the sill (for any sill thickness from 200 m to  $>1 \text{ km}$ ), the effect is minimal and is therefore ignored.

To better constrain the thickness of the sill, we calculate the density of the magma body in the months prior to eruption using estimates of the concentration of volatiles ( $\text{H}_2\text{O}$ ,  $\text{CO}_2$ ,  $\text{SO}_2$ ) supplied to the system and using solubility constraints to estimate the amount of exsolved gas in the magma at the pressure and temperature conditions expected in the shallow sill. The lavas erupted in 2005 were essentially aphyric (crystal-free) and as such, preclude melt inclusion

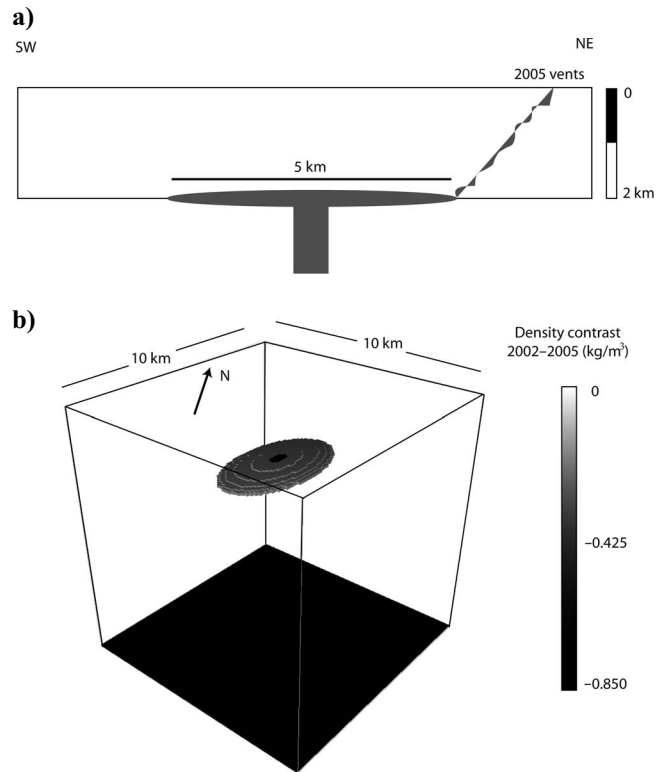


Figure 5. Simplified cross section through the caldera showing the location and geometry of the magma body in 2D (a) and 3D (b). (b) illustrates the geometry of the sill and the foam layer used to generate a maximum gravity anomaly of  $-874 \mu\text{Gal}$  (image from GRAV3D). The sill is  $5000 \times 3000 \times 700 \text{ m}$  and the foam layer is  $400 \times 800 \times 50 \text{ m}$ .

studies of the initial melt volatile content. However, melt inclusion data from the neighboring basaltic shield volcano, Fernandina (Figure 1), can be used to estimate the undegassed concentrations of volatiles feeding the shallow Sierra Negra system because Fernandina erupts lavas of very similar chemical composition to Sierra Negra (c.f., Reynolds et al., 1995; Allan and Simkin, 2000; Geist et al., 2008). The melt inclusions with the highest CO<sub>2</sub> content (~7000 ppm) represent the least degassed samples and have corresponding H<sub>2</sub>O contents of 0.8–1 wt.% and S contents of ~1600 ppm (Koleszar et al., 2007). The lithostatic pressure at the top of the magma chamber is ~58 MPa (2.2 km depth), a minimum for the system in part because we do not take into account the amount of magmatic overpressure (estimated at <15 MPa in 2005 from the amount of inflation; Yun et al., 2006). We estimate a magma temperature of 1150 °C based on the geothermometer developed by Montierth et al. (1995) for Mauna Loa basalts and using the composition of the tephra glass from the 2005 eruption (Geist et al., 2008).

The solubility of CO<sub>2</sub> in basalts at these conditions is lower than the amount of CO<sub>2</sub> dissolved in the melt phase entering the shallow chamber. Based on the solubility model of Newman and Lowenstern (2002), an input of 7000 ppm CO<sub>2</sub> into the system will degas to 265 ppm, releasing 6735 ppm of CO<sub>2</sub> into the gas phase. In contrast, the concentration of H<sub>2</sub>O in the melt is lower than its predicted solubility of 2.4 wt.% (Newman and Lowenstern, 2002), and therefore H<sub>2</sub>O would mostly remain in solution in a 2.2-km-deep sill. Determining the solubility of S in a basaltic magma is more complex because it involves more parameters, such as the composition of the melt and the oxygen fugacity. Based on the composition of the lava erupted during the 2005 eruption, the average oxygen fugacity of an ocean-island basalt (fayalite-magnetite-quartz buffer, Ballhaus, 1993; Gerlach, 1993), the pressure and temperature estimates mentioned earlier, and the models of Kilinc et al. (1983) and Wallace and Carmichael (1992), we obtain a S solubility of ~1600 ppm, suggesting S degassing would have been negligible at Sierra Negra prior to eruption. Based solely on the amount of CO<sub>2</sub> exsolved, the total weight percent of exsolved gas in the magma prior to the 2005 eruption is 0.7.

We do not take into account any compositional or temperature changes of the magma during storage in the magma chamber, which could cause H<sub>2</sub>O and S to saturate. We also do not take into account the possibility that H<sub>2</sub>O partially degasses with CO<sub>2</sub> in closed-system degassing (Dixon and Stolper, 1995), or that CO<sub>2</sub> is degassing from magma deeper within the system and that this gas is accumulating in the shallow magma chamber. Consequently, our estimate of the amount of gas exsolved in the sill is a minimum and the resulting estimate of the thickness of the sill is a maximum.

The estimate of the mass fraction of exsolved gas above yields a bulk magma density of 2500 kg/m<sup>3</sup>, calculated using a density of the molten silicate liquid of 2700 kg/m<sup>3</sup> and a gas density of 200 kg/m<sup>3</sup> (from the ideal gas law at the P, T of interest). Also note that this calculation is an average density and the amount of gas could be distributed heterogeneously in the magma reservoir (a possibility examined below).

The density of the magma body in 2002 is assumed to be that of the liquid with no exsolved gas or crystals (2700 kg/m<sup>3</sup>), based on evidence that the magma chamber was in a period of deflation and that magma withdrawal was occurring (Geist et al., 2006). The density contrast between June 2002 and 2005 is 200 kg/m<sup>3</sup>. Assuming no change in the planar geometry of the sill, we model the thickness of the sill required to produce the gravity anomaly recorded at SN09

during that time ( $-950 \pm 115 \mu\text{Gal}$ ). The best fit to the data is an 800-m-thick sill, illustrated in Figure 6.

We also explore the possibility that the magmatic gases were concentrated in a highly vesicular foam layer progressively accumulated at the top of the magma chamber between 2002 and 2005 (instead of being mixed uniformly in the sill). To obtain an independent estimate of the volume of this foam layer, we combine estimates of the total amount of SO<sub>2</sub> gas erupted during the eruption with estimates of the ratio of H<sub>2</sub>O/CO<sub>2</sub>/SO<sub>2</sub> in the melt feeding the system, to determine the volume of erupted gas, which we convert to its corresponding volume at depth. Given that a stable foam layer is <80 vol.% bubbles (Wilson et al., 1980), we use a conservative estimate of 50 vol.% porosity to calculate a total volume for the foam layer.

The total amount of SO<sub>2</sub> erupted over the eight days of the eruption is obtained from ozone monitoring instrument (OMI) satellite images and corresponds to  $\sim 1.9 \times 10^9$  kg (Simon Carn, personal communication). The H<sub>2</sub>O/CO<sub>2</sub>/S ratios in the undegassed magma are estimated from melt inclusion data from Fernandina (Koleszar et al., 2007) and correspond to an H<sub>2</sub>O/S ratio of 5.5 and a CO<sub>2</sub>/S ratio of 4.75. If we assume the ratios of the volatiles at depth prior to degassing are equivalent to the ratios in the eruptive plume and Fernandina volatile ratios are similar to those at Sierra Negra, then 45 wt.% of the plume gas composition was H<sub>2</sub>O, 40 wt.% was CO<sub>2</sub>, and 15 wt.% was SO<sub>2</sub>. The total amount of gas erupted equals  $11.6 \times 10^9$  kg, which translates to a volume of  $8.3 \times 10^9$  m<sup>3</sup> of gas at atmospheric pressure and temperature (calculated from the ideal gas law). Converted to a pressure of 58 MPa (corresponding to 2.2 km depth) at 1150 °C, the pre-eruptive volume of gas in the magma chamber is estimated at  $6.8 \times 10^7$  m<sup>3</sup>. Part of this volume will represent volatiles still dissolved in the melt prior to eruption, or exsolved but not accumulated in the foam layer. Therefore, the volume of the foam layer is considered a maximum value. Factoring in 50 vol.% porosity in the foam layer, the total volume of the layer is 13.6

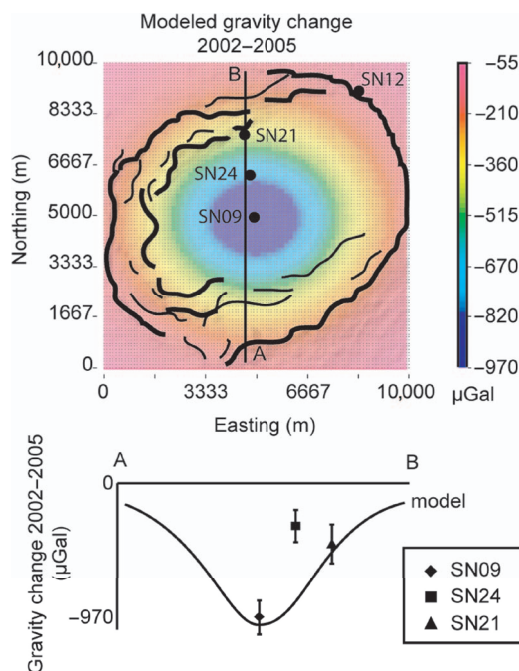


Figure 6. Modeled gravity change between June 2002 and 2005 caused by an 800-m-thick homogeneous sill with 10 vol.% vesiculation.

$\times 10^7 \text{ m}^3$ . This value serves as a rough estimate of the maximum volume of explosively erupted material. It is approximately equivalent to the volume of effusively erupted lava (Geist et al., 2008).

A two-layer sill was modeled so that the top of the foam layer was at 2.2 km depth, corresponding to the top of the magma chamber (Figure 5). The foam layer was assigned a density contrast of  $850 \text{ kg/m}^3$  (calculated from the porosity of the foam layer and the density of the erupted gas at the pressure and temperature conditions of the chamber) and the rest of the magma chamber had the same density contrast as in the first model,  $200 \text{ kg/m}^3$ . Because the volume of the foam layer is fixed, the area and thickness of the foam layer were varied along with the thickness of the underlying magma body until the maximum gravity signal produced most closely matched the signal observed between 2002 and 2005. The solution to this model is not unique and a 700-m-thick sill with a 50-m-thick foam layer ( $400 \times 800 \text{ m}$  area) will produce a comparable gravity signal to a thinner sill with a thicker or more extensive foam layer. Figure 7 shows the result of one of the configurations found to best fit our measured maximum residual gravity change for 2002–2005.

Although the modeling does not produce unique solutions to the geometry and the density of the shallow body beneath the caldera, it does produce solutions that are realistic and can explain the maximum residual gravity decrease between June 2002 and June 2005. The development of a foam layer with 50 vol.% vesiculation above a homogenous vesiculating magma body, or simply a thicker homogenous magma body with 10 vol.% vesiculation are both plausible conditions prior to the 2005 eruption, which was explosive in its opening phase. The formation of a foam layer was also put forward by Carbone et al. (2006, 2007) to explain the joint gravity decrease/tremor increase/pause in explosive activity at Mt. Etna during the 2002–2003 eruption, which resulted in a maximum residual gravity decrease of  $30 \text{ } \mu\text{Gal}$ , but no model was developed to quantify the ef-

fect. Studies at Masaya volcano have also shown a relationship between an increase in volatile supply and decrease in residual gravity (Williams-Jones et al., 2003).

The pattern of modeled residual gravity change with distance away from the center of deformation is gradual (Figures 6 and 7). This pattern suggests that station SN21, 1 km farther from the center of the caldera than SN24, should have experienced a smaller decrease in residual gravity than was observed. The actual variation in gravity change between 2002 and 2005 at these two stations is similar within error, suggesting that other factors not modeled may be affecting the gravity field on a smaller scale. The location of the 2005 eruptive vents on the northeast rim of the caldera (Geist et al., 2008), within  $\sim 2 \text{ km}$  of SN21 (Figure 2), and possible dike propagation from the sill to the surface might have caused localized gravity anomalies. Localized changes in the shallow hydrothermal system also cannot be ruled out. Given these potential complications, only the maximum change in residual gravity (station SN09) was used to fit the models.

Eight and twenty months after the eruption, the gravity signal at SN09 had returned to, and exceeded, the 2001–2002 levels (Figure 3) and was accompanied by a renewal of inflation but at a decelerating rate (Ruiz et al., 2007). The maximum  $\Delta g/\Delta h$  gradient during this time period plots above both the FAG and BCGAF gradients (Figure 4), suggesting the change in residual gravity after the eruption is caused by a mass and/or a density increase, both consistent with the loss of the gas-rich, crystal-poor magma during the eruption, leaving behind a denser, perhaps crystal-rich mush and renewed influx of relatively degassed magma from deeper in the system.

## CONCLUSIONS

Four-dimensional microgravity and deformation data at Sierra Negra volcano can be interpreted in terms of the subsurface processes responsible for the largest pre-eruptive inflation ever recorded at a basaltic caldera. The magnitude of maximum residual gravity change prior to the 2005 eruption ( $-950 \text{ } \mu\text{Gal}$ ) is also among the largest ever recorded. A gravity decrease of similar magnitude ( $-400 \text{ } \mu\text{Gal}$ ) was recorded by a permanent gravity station at the summit of the Mt. Etna volcano at the onset of the October 2002 eruption (Carbone et al., 2007). The duration of the anomaly was less than six hours and was interpreted as reflecting the opening of a dry fracture (not filled with magma)  $\sim 1 \text{ km}$  from the gravity measurement site. The duration of the gravity anomaly at Sierra Negra volcano is unknown because measurements were performed on only two consecutive days over periods of 15–20 minutes each time. This problem illustrates the need for continuous 4D gravity monitoring at active volcanoes (Williams-Jones et al., 2008) but the logistical limitations, combined with the current technology available for continuous microgravity recordings, make this unfeasible at Sierra Negra volcano. However, based on the time gap between the gravity measurement in June 2005 and the onset of the eruption in October 2005, we do not attribute the gravity decrease to the opening of a fracture.

Vesiculation of the magma as the volatiles reached their saturation point can explain the simultaneous uplift of the caldera floor and the decrease in gravity observed between 2001–2002 and June 2005. Although the proposed models do not offer unique solutions, geochemical constraints on the amount of gas present in the magma chamber prior to eruption allow us to model the thickness of the magma body required to produce the observed residual gravity variations. Al-

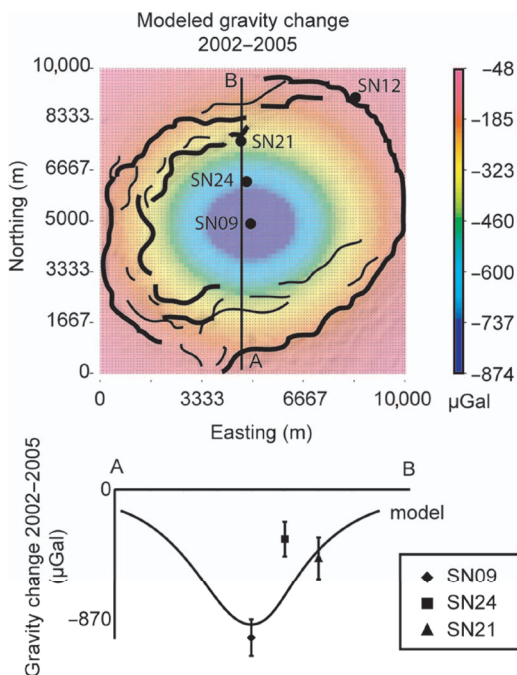


Figure 7. Modeled gravity change between June 2002 and 2005 caused by a 700-m-thick sill with 10 vol.% vesiculation and a 50-m-thick foam layer with 50 vol.% vesicularity at the top.

though the error associated with these estimates is large, the models provide a first-order constraint on the third dimension of the shallow magma reservoir at Sierra Negra.

Modeling of the time-series data also offers insight into the time-scales of vesiculation at Sierra Negra and can be used to estimate the volume of gas in the magma chamber prior to eruption. Faulting events at Sierra Negra in the years and months leading up to the 2005 eruption potentially allowed for a partial release of pressure in the subsurface magma body and accommodation of subsurface volume expansion. The onset of vesiculation sometime between June 2002 and June 2005 is associated with the accelerating rate of inflation recorded from April 2003 to October 2005 (Chadwick et al., 2006), and might have ultimately triggered the eruption. The cause for the onset of vesiculation might have been the influx of volatile-rich magma from depth, combined with chemical evolution of the melt in the chamber (volatile phases reaching saturation) and perhaps a sudden, partial release of pressure during the April 16, 2005 faulting event.

### ACKNOWLEDGMENTS

The authors would like to thank the Galápagos National Park for their permission and assistance in the field and the Charles Darwin Research Station for their logistical help. We also thank Ayline Llona for her assistance in providing Dan Johnson's gravity data. Discussions with Paul Wallace helped clarify issues on S solubility. Support was provided by NSF grant EAR0538205 to the University of Idaho and an NSERC Discovery Grant to Glyn Williams-Jones. PMEL contribution number 3193.

### REFERENCES

- Allan, J. F., and T. Simkin, 2000, Fernandina volcano's evolved, well-mixed basalts: Mineralogical and petrological constraints on the nature of the Galapagos plume: *Journal of Geophysical Research — Solid Earth*, **105**, 6017–6041.
- Amelung, F., S. Jónsson, H. Zebker, and P. Segall, 2000, Widespread uplift and "trapdoor" faulting on Galápagos volcanoes observed with radar interferometry: *Nature*, **407**, 993–996.
- Ballhaus, C., 1993, Redox states of lithospheric and asthenospheric upper-mantle: *Contributions to Mineralogy and Petrology*, **114**, 331–348.
- Battaglia, M., C. Roberts, and P. Segall, 1999, Magma intrusion beneath Long Valley caldera confirmed by temporal changes in gravity: *Science*, **285**, 2119–2122.
- Battaglia, M., P. Segall, and C. Roberts, 2003, The mechanics of unrest at Long Valley caldera, California: 2. Constraining the nature of the source using geodetic and micro-gravity data: *Journal of Volcanology and Geothermal Research*, **127**, 219–245.
- Berrino, G., G. Corrado, G. Luongo, and B. Toro, 1984, Ground deformation and gravity changes accompanying the 1982 Pozzuoli uplift: *Bulletin of Volcanology*, **47**, 187–200.
- Carbone, D., G. Budetta, F. Greco, and L. Zuccarello, 2007, A data sequence acquired at Mt. Etna during the 2002–2003 eruption highlights the potential of continuous gravity observations as a tool to monitor and study active volcanoes: *Journal of Geodynamics*, **43**, 320–329.
- Carbone, D., L. Zuccarello, G. Saccorotti, and F. Greco, 2006, Analysis of simultaneous gravity and tremor anomalies observed during the 2002–2003 Etna eruption: *Earth and Planetary Science Letters*, **245**, 616–629.
- Chadwick, W. W., D. J. Geist, S. Jónsson, M. Poland, D. J. Johnson, and C. M. Meertens, 2006, A volcano bursting at the seams: Inflation, faulting, and eruption at Sierra Negra volcano, Galápagos: *Geology*, **34**, 1025–1028.
- Dixon, J. E., and E. M. Stolper, 1995, An experimental study of water and carbon dioxide solubilities in mid-ocean ridge basaltic liquids: 2. Applications to degassing: *Journal of Petrology*, **36**, 1633–1646.
- Geist, D., W. Chadwick, and D. Johnson, 2006, Results from new GPS and gravity monitoring networks at Fernandina and Sierra Negra Volcanoes, Galápagos, 2000–2002: *Journal of Volcanology and Geothermal Research*, **150**, 79–97.
- Geist, D. J., K. S. Harpp, T. R. Naumann, M. Poland, W. W. Chadwick, M. Hall, and E. Rader, 2008, The 2005 eruption of Sierra Negra volcano, Galápagos, Ecuador: *Bulletin of Volcanology*, **70**, 655–673.
- Gerlach, T. M., 1993, Oxygen buffering of Kilauea volcanic gases and the oxygen fugacity of Kilauea basalt: *Geochimica et Cosmochimica Acta*, **57**, 795–814.
- Gottsmann, J., L. Wooller, J. Martí, J. Fernández, A. G. Camacho, P. J. Gonzalez, A. Garcia, and H. Rymer, 2006, New evidence for the reawakening of Tiede volcano: *Geophysical Research Letters*, **33**, L20311.
- GRAV3D; A program library for forward modeling and inversion of gravity data over 3D structures, version 20070309, 2007, developed under the consortium research project Joint/Cooperative Inversion of Geophysical and Geological Data: UBC-Geophysical Inversion Facility, Department of Earth and Ocean Sciences, The University of British Columbia, Vancouver.
- Johnson, D. J., 1992, Dynamics of magma storage in the summit reservoir of Kilauea volcano, Hawaii: *Journal of Geophysical Research — Solid Earth*, **97**, 1807–1820.
- Jousset, P., S. Dwipa, F. Beauducel, T. Duquesnoy, and M. Diament, 2000, Temporal gravity at Merapi during the 1993–1995 crisis: An insight into the dynamical behavior of volcanoes: *Journal of Volcanology and Geothermal Research*, **100**, 289–320.
- Kauahikaua, J., and A. Miklius, 2003, Long-term trends in microgravity at Kilauea's summit during the Pu'u'ū'ū-Kupaianaha eruption: U. S. Geological Survey Professional Paper **1676**, 165–171.
- Kilinc, A., I. S. E. Carmichael, M. L. Rivers, and R. O. Sack, 1983, The ferric-ferrous ratio of natural silicate liquids equilibrated in air: *Contributions to Mineralogy and Petrology*, **83**, 136–140.
- Koleszar, A. M., A. E. Saal, E. H. Hauri, and M. D. Kurz, 2007, Melt inclusions from the Galapagos plume: Mirrors and mirages of the deep: *Geochimica et Cosmochimica Acta*, **71**, A508–A508.
- Lipman, P. W., 1997, Subsidence of ash-flow calderas: Relation to caldera size and magma-chamber geometry: *Bulletin of Volcanology*, **59**, 198–218.
- Montieth, C., A. D. Johnston, and K. V. Cashman, 1995, An empirical glass-composition-based geothermometer for Mauna Loa lavas, in *Mauna Loa revealed: Structure, composition, history, and hazards: Geophysical Monograph*, **92**, 207–217.
- Newman, S., and J. B. Lowenstern, 2002, VOLATILECALC: A silicate melt-H<sub>2</sub>O-CO<sub>2</sub> solution model written in Visual Basic for Excel: *Computers & Geosciences*, **28**, 597–604.
- Reynolds, R., D. Geist, and M. Kurz, 1995, Physical volcanology and structural development of Sierra Negra volcano, Galápagos Archipelago: *Geological Society of America Bulletin*, **107**, 1398–1410.
- Ruiz, A., D. Geist, and W. Chadwick, 2007, Inflation of Sierra Negra volcano since the 2005 eruption: *Eos: Transactions, AGU*, V53C–1422.
- Rymer, H., 1996, Microgravity monitoring, in R. Scarpa, and R. I. Tilling, eds., *Monitoring and mitigation of volcano hazards: Springer-Verlag*, 169–198.
- Rymer, H., and G. Brown, 1989, Gravity changes as a precursor to volcanic eruption at Poas volcano, Costa Rica: *Nature*, **342**, 902–905.
- Rymer, H., and G. Williams-Jones, 2000, Volcanic eruption prediction: Magma chamber physics from gravity and deformation measurements: *Geophysical Research Letters*, **27**, 2389–2392.
- Tsuboi, C., 1983, *Gravity: G. Allen and Unwin*.
- Wallace, P., and I. S. E. Carmichael, 1992, Sulfur in basaltic magmas: *Geochimica et Cosmochimica Acta*, **56**, 1863–1874.
- Williams-Jones, G., H. Rymer, G. Mauri, J. Gottsmann, M. Poland, and D. Carbone, 2008, Towards continuous 4D microgravity monitoring of volcanoes: *Geophysics*, this volume.
- Williams-Jones, G., H. Rymer, and D. A. Rothery, 2003, Gravity changes and passive SO<sub>2</sub> degassing at the Masaya caldera complex, Nicaragua: *Journal of Volcanology and Geothermal Research*, **123**, 137–160.
- Wilson, L., R. S. J. Sparks, and G. P. L. Walker, 1980, Explosive volcanic eruptions — IV: The control of magma chamber and conduit geometry on eruption column behavior: *Geophysical Journal of the Royal Astronomical Society*, **63**, 117–148.
- Wood, C., 1984, Calderas: A planetary perspective: *Journal of Geophysical Research*, **89**, 8391–8406.
- Yokoyama, I., and H. Tajima, 1957, A gravity survey on Volcano Mihara, Ooshima Island by means of a Worden gravimeter: *Bulletin of the Earthquake Research Institute*, **35**, 23–33.
- Yun, S.-H., P. Segall, and H. A. Zebker, 2006, Constraints on magma chamber geometry at Sierra Negra Volcano, Galápagos Islands, based on InSAR observations: *Journal of Volcanology and Geothermal Research*, **150**, 232–243.